

The Cosmic Evolution Survey (COSMOS) – Overview

N. Scoville^{1,2}, H. Aussel¹⁷, M. Brusa⁵, P. Capak¹, C. M. Carollo⁸, M. Elvis³, M. Giavalisco⁴, L. Guzzo¹⁵, G. Hasinger⁵, C. Impey⁶, J.-P. Kneib⁷, O. LeFevre⁷, S. J. Lilly⁸, B. Mobasher⁴, A. Renzini^{9,19}, R. M. Rich¹⁸, D. B. Sanders¹⁰, E. Schinnerer^{11,12}, D. Schminovich¹³, P. Shopbell¹, Y. Taniguchi¹⁴, N. D. Tyson¹⁶

*Based on observations with the NASA/ESA *Hubble Space Telescope*, obtained at the Space Telescope Science Institute, which is operated by AURA Inc, under NASA contract NAS 5-26555; also based on data collected at : the Subaru Telescope, which is operated by the National Astronomical Observatory of Japan; the XMM-Newton, an ESA science mission with instruments and contributions directly funded by ESA Member States and NASA; the European Southern Observatory under Large Program 175.A-0839, Chile; Kitt Peak National Observatory, Cerro Tololo Inter-American Observatory, and the National Optical Astronomy Observatory, which are operated by the Association of Universities for Research in Astronomy, Inc. (AURA) under cooperative agreement with the National Science Foundation; the National Radio Astronomy Observatory which is a facility of the National Science Foundation operated under cooperative agreement by Associated Universities, Inc ; and the Canada-France-Hawaii Telescope with MegaPrime/MegaCam operated as a joint project by the CFHT Corporation, CEA/DAPNIA, the NRC and CADC of Canada, the CNRS of France, TERAPIX and the Univ. of Hawaii.

¹California Institute of Technology, MC 105-24, 1200 East California Boulevard, Pasadena, CA 91125

²Visiting Astronomer, Univ. Hawaii, 2680 Woodlawn Dr., Honolulu, HI, 96822

³Harvard-Smithsonian Center for Astrophysics, 60 Garden Street, Cambridge, MA 02138

⁴Space Telescope Science Institute, 3700 San Martin Drive, Baltimore, MD 21218

⁵Max Planck Institut für Extraterrestrische Physik, D-85478 Garching, Germany

⁶Steward Observatory, University of Arizona, 933 North Cherry Avenue, Tucson, AZ 85721

⁷Laboratoire d’Astrophysique de Marseille, BP 8, Traverse du Siphon, 13376 Marseille Cedex 12, France

⁸Department of Physics, ETH Zurich, CH-8093 Zurich, Switzerland

⁹European Southern Observatory, Karl-Schwarzschild-Str. 2, D-85748 Garching, Germany

¹⁰Institute for Astronomy, 2680 Woodlawn Dr., University of Hawaii, Honolulu, Hawaii, 96822

¹¹National Radio Astronomy Observatory, P.O. Box 0, Socorro, NM 87801-0387

¹²Max Planck Institut für Astronomie, Königstuhl 17, Heidelberg, D-69117, Germany

¹³Department of Astronomy, Columbia University, MC2457, 550 W. 120 St. New York, NY 10027

¹⁴Astronomical Institute, Graduate School of Science, Tohoku University, Aramaki, Aoba, Sendai 980-8578, Japan

¹⁵INAF-Osservatorio Astronomico di Brera, via Bianchi 46, I-23807 Merate (LC), Italy

¹⁶American Museum of Natural History, Central Park West at 79th Street, New York, NY 10024

¹⁷Service d’Astrophysique, CEA/Saclay, 91191 Gif-sur-Yvette, France

¹⁸Department of Physics and Astronomy, University of California, Los Angeles, CA 90095

¹⁹Dipartimento di Astronomia, Universit di Padova, vicolo dell’Osservatorio 2, I-35122 Padua, Italy

ABSTRACT

The Cosmic Evolution Survey (COSMOS) is designed to probe the correlated evolution of galaxies, star formation, active galactic nuclei (AGN) and dark matter (DM) with large-scale structure (LSS) over the redshift range $z > 0.5$ to 6. The survey includes multi-wavelength imaging and spectroscopy from X-ray to radio wavelengths covering a $2 \square^\circ$ area, including HST imaging. Given the very high sensitivity and resolution of these datasets, COSMOS also provides unprecedented samples of objects at high redshift with greatly reduced cosmic variance, compared to earlier surveys. Here we provide a brief overview of the survey strategy, the characteristics of the major COSMOS datasets, and summarize the science goals.

Subject headings: cosmology: observations — cosmology: large scale structure of universe — cosmology: dark matter — galaxies: formation — galaxies: evolution — surveys

1. Introduction

Our understanding of the formation and evolution of galaxies and their large-scale structures (LSS) has advanced enormously over the last decade – a result of a phenomenal synergy between theoretical and observational efforts. Deep observational studies using the Hubble Space Telescope (HST) and the largest ground based telescopes have probed galaxy and AGN populations back to redshift $z = 6$ when the universe had aged less than 1 billion of its current 13 billion years. Just as remarkable is the enormous success of numerical simulations for Λ CDM models in reproducing many of the current LSS characteristics, all starting from an initial, nearly uniform, hot universe.

The Hubble Deep Field (HDF-N & S), GOODS and UDF have provided exquisite imaging of galaxy populations in narrow cones out to $z \sim 5 - 6$ (Williams et al. 1996, 2000; Giavalisco et al. 2004; Beckwith et al. 2006). Ground based multi-band imaging and spectroscopy provide redshifts and hence cosmic ages for these populations. Most briefly, the early universe galaxies were more irregular/interacting than at present and the overall cosmic star formation rate probably peaked at $z \sim 1 - 3$ with 10 - 30 times the current rates (Lilly et al.

1996; Madau et al. 1996; Cary & Elbaz 2001). Although some large scale structure and clustering of the luminous, high redshift galaxies is in evidence (e.g. Ettori et al. 2004; Mei et al. 2006), it is the theoretical simulations which have best characterized (or at least hypothesized) the larger scale, dark matter structure (e.g. Benson et al. 2001; Springel et al. 2006). In fact, the major gap which exists in our current understanding is the coupling between the LSS and the evolution of luminous galaxies – specifically, their assembly via merging and their star formation and AGN fueling, both probably also linked to galactic interactions and mergers (e.g. Hernquist & Springel 2003).

The COSMOS survey is the first survey encompassing a sufficiently large area that it can address the coupled evolution of LSS, galaxies, star formation and AGN. COSMOS is the largest HST survey ever undertaken – imaging an equatorial, $\sim 2\text{°}$ field with single-orbit I-band exposures to a point source depth of $I_{AB} = 28$ mag and 50% completeness for galaxies $0.5''$ in diameter at $I_{AB} = 26.0$ mag (5σ , Scoville et al. 2006a). Extensive multi- λ ground and space-based observations of this field (see Section 4) have been gathered or are anticipated, spanning the entire spectrum from X-ray, UV, optical/IR, mid-infrared, mm/submm and to radio with extremely high sensitivity imaging and spectroscopy (Hasinger et al. 2006; Taniguchi et al. 2006; Capak et al. 2006; Lilly et al. 2006; Impey et al. 2006; Sanders et al. 2007; Bertoldi et al. 2006; Schinnerer et al. 2006). This full spectrum approach is required to probe the coupled evolution of young and old stellar populations, starbursts, the ISM (molecular and ionized components), AGN and dark matter. The multi- λ approach is also necessitated by the fact that light from different cosmic epochs is differentially redshifted and the presence of dust obscuration in many of the most rapidly-evolving galactic regions. The large areal coverage of COSMOS is motivated to sample the largest structures existing in the local universe since smaller area coverage leads to severe cosmic variance.

COSMOS will detect $\simeq 2 \times 10^6$ galaxies and AGN (see Table 1), sampling a volume in the high redshift universe approaching that sampled locally by the Sloan Digital Sky Survey (SDSS). In this article, we provide a brief overview of the scientific goals of the COSMOS survey and an overall summary of the survey observational program, providing an introduction to the subsequent articles in this journal which provide more detailed description of the separate observational programs and the initial science results, based on the first 2 years of the survey.

2. COSMOS Science Goals

The COSMOS survey addresses nearly every aspect of observational cosmology over the majority of the Hubble time, out to $z \sim 6$:

- the assembly of galaxies, clusters and dark matter on scales up to $\geq 2 \times 10^{14} M_{\odot}$;
- reconstruction of the dark matter distributions and content using weak gravitational lensing at $z < 1.5$;
- the evolution of galaxy morphology, galactic merger rates and star formation as a function of LSS environment and redshift;
- evolution of AGN and the dependence of black hole growth on galaxy morphology and environment; and
- the mass and luminosity distribution of the earliest galaxies, AGN and intergalactic gas at $z = 3$ to 6 and their clustering.

The growth of galaxies, AGN and dark matter structure is traced in COSMOS over a period corresponding to $\sim 75\%$ of the age of the universe. For reference, we show in Figure 1 the comoving volume and differential volumes sampled by COSMOS as a function of z , together with the age and lookback times. The largest survey of the local universe (SDSS) samples approximately $3 \times 10^7 h^{-3} \text{ Mpc}^3$ at $z \leq 0.1$ (SDSS web page); COSMOS samples equivalent or larger volumes in the early universe (see Figure 1).

The expected numbers of different types of objects in the 2arcmin^2 field at the COSMOS sensitivities are given in Table 1. Over 2 million galaxies are detected in the HST-ACS and Subaru optical imaging and photometric redshifts have been determined for approximately 800,000 galaxies (Mobasher et al. 2006). The COSMOS spectroscopic surveys (VLT and Magellan; Lilly et al. (2006); Impey et al. (2006)) will yield $\sim 40,000$ galaxies with accurate redshifts at $z = 0.5 - 2.5$, all having $0.05''$ HST imaging. Redshift bins can then be constructed, each with thousands of galaxies, to probe evolution of the morphological distribution (E, Sp, Irr, etc.) as a function of both LSS and time. Each redshift slice of width $\Delta z \simeq 0.02$ (fine enough to resolve structures along the line of sight, see Figure 2) will have 500 – 1000 galaxies. Evolution of the luminosity and spatial correlation functions for type-selected galaxies can be analyzed with unprecedented statistical accuracy.

2.1. Large Scale Structure

Figure 2 shows the results of a LSS Λ -CDM simulation for $z = 1$ and 2 (Virgo Consortium; Frenk et al. (2002)). The gray scale shows the dark matter distributions and the dots represent galaxies chosen by semi-analytic techniques to populate the DM halos. Observational studies of Lyman break galaxies and deep X-ray imaging with CXO/XMM are broadly consistent with these models with respect to the LSS (Giavalisco et al. 1998; Adelberger et al.

1998; Gilli et al. 2003).

The need to sample very large scales arises from the fact that structure occurs on mass scales up to $\geq 10^{14}M_{\odot}$ and existing smaller, contiguous surveys (see Figure 2) are likely to be unrepresentative at $z \sim 1$. This is illustrated in Figure 3, which shows the probability of enclosing a given mass as a function of field size. Earlier projects, such as GOODS (Giavalisco et al. 2004) and GEMS (Rix et al. 2004), adequately sample masses up to $3 \times 10^{13}M_{\odot}$, whereas COSMOS samples the largest expected structures at $\sim 2 \times 10^{14}M_{\odot}$ (dark and luminous matter). The evolution of the halo and cluster mass distribution is shown in the right panel of Figure 3 – dramatically demonstrating the evolution of the dark matter on scales probed by COSMOS. Evolution of the luminous-galaxy occupation number in halos as a function of both redshift and halo mass can provide stringent tests of LSS models. COSMOS yields critical data on the efficiency of star formation as a function of environment and cosmic epoch.

2.2. Gravitational Lensing and Dark Matter

The small distortions to the shapes of background galaxies resulting from weak gravitational lensing by foreground structures depend on the distribution of dark matter as characterized by the evolution of its power spectrum $P(k, z)$ (Kaiser et al. 1995; Mellier 1999; Refregier 2003). The reliability of the derived results depends on the dispersion of the intrinsic shapes of the background sources, instrumental PSFs and the number of background, lensed galaxies and their redshifts. The ACS PSF permits extraction of shapes for ~ 87 galaxies per arcmin², 2-3 times more than the number in the best ground-based data (Park et al. 2004; Rhodes et al. 2006). Resulting dark matter maps thus have much higher fidelity and improved sensitivity (down to $10^{13}M_{\odot}$). The observed distributions of halo masses can then be compared with the theoretically predicted evolution as a function of redshift over the range 10^{13} to $2 \times 10^{14} M_{\odot}$ (Bahcall et al. 2004).

2.3. Assembly and Evolution of Galaxies

Galaxies in the early universe are built up by two major processes: dissipative collapse and merging of lower mass protogalactic and galactic components. Their intrinsic evolution is then driven by the conversion of primordial and interstellar gas into stars, with galactic merging and interactions triggering star formation and starbursts. While there is general agreement over this qualitative picture, the precise timing of these events, as well as their

relation to local environment, remains to be observationally explored. For example, the assembly of massive galaxies apparently takes place at a substantially earlier epochs ($z > 2$) than predicted in the earlier semi-analytic models. Spheroids include the majority of the stellar mass in the local universe (Fukugita, Hogan & Peebles 1998), and may have formed at very early times ($z > 2 - 3$ (Renzini 2006; Peebles 2002; Bell et al. 2004). Their progenitors at $z \sim 3$ are possibly detected as Lyman-break galaxies (Adelberger et al. 2005) and/or SCUBA sources (Eales et al. 1999; Blain et al. 2004). The Gemini Deep Deep Survey (Glazebrook et al. 2004) and K20 Survey (Ciamatti et al. 2004) find massive, passively evolving galaxies out to $z \sim 2$; The Gemini Deep Survey finds massive galaxies out to $z \sim 2$; HDF-N has few massive galaxies and those in the HDF-S are at higher z , suggesting strong environmental dependence and underscoring the need for large fields. As for spiral galaxies, their major epoch of formation may be in the range $z = 1 - 2$ (Ferguson et al. 2000; Conselice et al. 2004).

3. COSMOS Field Selection

The COSMOS field is located near the celestial equator to ensure visibility by all astronomical facilities, especially unique instruments such as the next generation 20 – 30m optical/IR telescope(s). The time requirements for deep imaging and spectroscopy over a total area of $2\pi^\circ$, containing over a million galaxies makes it strategically imperative that the field be readily observable by all large optical/IR telescopes. For radio studies, high-declination fields such as Lockman Hole, HDF-North, Groth strip and CDF-South are ruled out – they can not be easily observed by *both* (E)VLA in the north and ALMA in the south.

The COSMOS field is a $1.4^\circ \times 1.4^\circ$ square, aligned E-W, N-S, centered at RA = 10:00:28.6, DEC = +02:12:21.0 (J2000). (The field is near to, but offset from the RA = 10 hr VVDS field.) The field is devoid of bright X-ray, UV, and radio sources. Relative to other equatorial fields, COSMOS has exceptionally *low and uniform Galactic extinction* ($\langle E_{(B-V)} \rangle \simeq 0.02$ mag).

3.1. IR Backgrounds

The most serious concern for equatorial, survey fields is that they have somewhat higher IR backgrounds than the most favorable high Galactic and ecliptic latitude fields. In Table 2, we tabulate the backgrounds and comparative sensitivities (5σ) for COSMOS, SWIRE/XMM (another equatorial field), and the lowest background, high declination fields such as Lock-

man Hole, CDF-S, HDF-N, and Groth Strip (which all have similar backgrounds). For the COSMOS field, we use the background appropriate to the time when it is observed by Spitzer; for the other fields we have use their minimum background estimates. For the COSMOS field, the mean $100\mu\text{m}$ background is 0.90 MJy sr^{-1} , compared to $\sim 0.45 \text{ MJy sr}^{-1}$ in the very best, non-equatorial fields such as Lockman Hole. However, the sensitivity for a given integration time, scales as the square root of the background emission. Therefore, the lowest background fields (Lockman Hole, CDF-S, HDF-N, and Groth Strip) will have only $\sim 15 - 25\%$ better sensitivity than COSMOS for equivalent integration times (Table 2). This small reduction in sensitivity, associated with selection of an equatorial field, was deemed as an acceptable compromise when weighed against the inaccessibility of higher declination fields to the unique ground-based facilities.

4. COSMOS Multi-wavelength Surveys

The COSMOS field is accessible to essentially all astronomical facilities, enabling complete multi- λ datasets (x-ray, UV, optical/IR, FIR/submm to radio). The status of these observational programs is summarized in Table 3, and on the COSMOS web-site ([\protecthttp://www.astro.caltech.edu/~cosmos/](http://www.astro.caltech.edu/~cosmos/)). The extensive allocations on Subaru, CFHT, UKIRT and NOAO have providing extremely deep photometry for 12 bands from U to K_s , enabling accurate photo-z's, integrated colors and color selection of populations (e.g. LBGs, EROs, AGN, etc) for essentially all objects detected in the 2M° ACS field. The photometry catalogs from these data contain over 2 million objects at $<27 \text{ mag}$ (AB) in the U to K_s bands. The initial photometric redshift catalog has 860,000 objects at $<25 \text{ mag}$ (i-band) (Mobasher et al. 2006). The ground-based imaging is an on-going effort, currently directed toward obtaining narrow and intermediate width filter imaging with Subaru SuprimeCam (for more accurate redshifts and detection of high-z emission line objects) and deeper near-infrared imaging at UKIRT, CFHT, and UH88.

A very large VLT/VIMOS program (z-COSMOS) will provide spectra and redshifts for $\geq 30,000$ galaxies up to $z \sim 3$ (Lilly et al. 2006). A second spectroscopy program, focussed towards the AGN population and red objects, is being conducted on Magellan/IMACS (Impey et al. 2006). The VLT and Magellan spectroscopy is expected to complete within ~ 3 years.

XMM has devoted 1.4 Ms to a complete X-ray survey of the field (Hasinger et al. 2006), and COSMOS was one of the deep-GALEX fields for UV imaging (Schiminovich et al. 2006). The VLA-COSMOS survey was allocated 275(+60) hrs for the largest, deep wide field image every done at arcsec resolution (Schinnerer et al. 2006). The XMM, GALEX and VLA

surveys are all now complete. Deep mid-infrared observations (IRAC) and shallower far-infrared observations (MIPS) of the full COSMOS field have been obtained with Spitzer (see Table 3, Sanders et al. (2007)). At mm/submm-wavelengths, partial surveys of COSMOS are on-going at the IRAM-30m and CSO telescopes (Bertoldi et al. 2006; Aguirre et al. 2006).

5. Major Observational Goals

In this section, we briefly review the major ingredients of the COSMOS survey.

5.1. Galaxy Redshifts : Photometric and Spectroscopic

Determining the redshifts or lookback time of individual galaxies is clearly one of the most difficult and time consuming aspects of any cosmological evolution survey. In COSMOS this is even more difficult since the redshifts are needed with sufficient precision not just to determine the cosmic epoch, but also to place the galaxies within (or outside) structures along the line of sight. Without high precision, structures become 'blurred' due to scattering of galaxies to different distances in the line of sight and for specific galaxies, their environment cannot be determined. The accuracy of redshifts required for the environmental specification is $\Delta z/(1+z) \leq 0.02$ based on LSS simulations such as shown in Figure 2; lower precision degrades the LSS/environmental definition.

In COSMOS, photometric redshifts (Mobasher et al. 2006) are obtained from deep (mostly ground-based) imaging – from Subaru (Taniguchi et al. 2006), CFHT, UKIRT, and NOAO (Capak et al. 2006). At present the photometric-redshift accuracy is $\sigma_z/(1+z) \sim 0.04$ for approximately 2×10^5 galaxies at $z < 1.2$ (and 0.1 accuracy for 8×10^5 galaxies), enabling initial definition of the LSS, especially for the denser environments (Scoville et al. 2006b; Finoguenov et al. 2006). Expected improvements in the sensitivity of the near infrared imaging and the addition of more bands should further increase the accuracy and increase the redshift range of the photometric redshifts within the next year.

Very large spectroscopic surveys are now ongoing as part of COSMOS at the VLT and Magellan telescopes (Lilly et al. 2006; Impey et al. 2006). The spectroscopic sample will eventually include approximately 37,500 galaxies and several thousand AGN down to limits of $I_{AB} = 24.5$. The zCOSMOS spectroscopy provides precision of ~ 0.0003 in redshift for the brighter objects at $z < 1.2$ and somewhat lower precision for the fainter objects. These spectroscopic samples will provide very precise definition of the environment, albeit for smaller subsets of the overall COSMOS galaxy population.

5.2. Galaxy Evolution : HST Imaging and SEDs

The evolutionary status of galaxies can be analyzed from either their morphologies or their spectral energy distributions (SED, characterizing the stellar population).

Morphological parameters for the galaxies are obtained from the HST imaging (e.g. bulge/disk ratios, concentration, asymmetry, size, multiplicity, clumpiness) (Scarlata et al. 2006; Cassata et al. 2006; Capak et al. 2006a). The COSMOS I-band ACS images have sufficient depth and resolution to allow classical bulge-disk decomposition for L^* galaxies at $z \leq 2$, while less detailed structural parameters such as compactness, asymmetry, clumpiness and size can be measured for all galaxies down to the spectroscopic limit ($I_{AB} \sim 25$), out to $z \sim 5$. None of these measures can be obtained from ground-based imaging at these flux levels; ACS imaging has been a critical ingredient for understanding the evolution and build-up of galaxies.

In COSMOS, deep imaging (from Subaru, GALEX, UKIRT and NOAO, and SPITZER-IRAC) provides SEDs to characterize the integrated stellar populations of the 1-2 million galaxies detected with HST. The rest-frame SEDs are derived self-consistently with the photometric redshift determinations. (For most of the galaxies, the multi-color imaging has insufficient resolution to measure internal population or extinction gradients.)

5.3. Environment : Galaxy Overdensities, DM Weak Lensing and Correlation Functions

The environment or LSS in which a given galaxy resides might be defined from the local number density of galaxies or from the DM density as determined from weak lensing or the galaxy-galaxy velocity dispersion. The COSMOS HST imaging provides measures of the close-in environment (from galaxy multiplicity and merger indicators such as tidal distortions) and larger-scale DM environment (from weak lensing shear analysis, Massey et al. 2006). As noted in Section 5.1, definition of the environment is critically dependent on moderately high accuracy spectroscopic (or photometric) redshifts; the integrated, multi-wavelength approach adopted for COSMOS is intended to maximize the impact and utility of each component. Having multiple approaches to environmental determination will provide added confidence in the LSS definition. An example of this is the use of diffuse X-ray emission as detected in the XMM-COSMOS survey to identify and confirm galaxy groups and clusters (Finoguenov et al. 2006).

The wide-area, uniform ACS and Subaru COSMOS surveys allow determination of spatial correlation functions as a function of type (morphological and SED) and luminosity

and their evolution with redshift and environment. The enormous sizes of the samples which become available in COSMOS enable precision approaching that of SDSS but at much higher redshift. Clustering of different populations of galaxies, probed by the correlation function, is related to the distribution of underlying dark matter from weak lensing. COSMOS provides over a hundred slices of the universe back to $z \sim 2$ to reveal the spatial distribution and shapes of tens of thousands of galaxies sampling the full range of cosmic structure.

5.4. Activity : Starbursts and AGN

The COSMOS survey samples $\sim 45,000$ galaxies spectroscopically – providing an enormous sample of emission line tracers of both starbursts and AGN over a broad range of redshift. In addition, complete very high sensitivity radio continuum (VLA; Schinnerer et al. 2006) and X-ray (XMM; Hasinger et al. 2006) coverage, directly probes the population of AGN; the radio continuum sensitivity allows the detection of the very luminous starburst populations out to a redshift of ~ 1.5 and the most luminous systems out to $z \sim 3$. Less luminous radio galaxies (type FRI) could be seen out to $z \sim 5$. Coverage with Spitzer MIPS detects dust embedded ultraluminous starbursts and AGN out to $z \sim 2 - 3$ (Sanders et al. 2007). COSMOS includes large samples of galaxies with multiple, independent tracers of luminous activity. These can be analyzed as a function of both redshift and environment, opening up fundamental investigations of starburst and AGN fueling in the early universe.

mm/submm- λ surveys of the COSMOS field have been initiated to identify the most luminous starbursts at $z > 1$ (Bertoldi et al. 2006; Aguirre et al. 2006). In the long term, high resolution imaging with ALMA will be a vital capability – providing resolved images of the neutral ISM, luminosity distribution and dynamical masses for virtually all COSMOS galaxies having ISMs equivalent to the Galaxy. The COSMOS field was specifically selected to ensure ALMA access (see Section 3).

5.5. $z = 3 - 6$: High Redshift Galaxies, LSS and IGM

The large areal coverage and high sensitivity of the COSMOS survey provides significant samples of $z > 3$ objects, selected by multi-band color criteria, the Lyman-break method (Giavalisco et al. 2006), or by direct detection of Ly α emission lines (Ajiki et al. 2006). At these higher redshifts, the field subtends over 200 Mpc (comoving) and samples a volume similar to that sampled locally by SDSS.

6. COSMOS Data Archives and Websites

Table 4 list URLs for the COSMOS survey. The major COSMOS datasets become publicly available in staged releases (following calibration and validation) through the web site for IPAC/IRSA : <http://irsa.ipac.caltech.edu/data/COSMOS/> . The COSMOS HST data is also available at STScI-MAST : <http://archive.stsci.edu/>. Archives are also maintained at INAF - IASF (<http://cosmosdb.mi.iasf.cnr.it> and Observatoire de Marseille (<http://cencosw.oamp.fr/EN/index.en.html>) in Europe. These archives include calibrated image and spectral data and catalogs when they are each released (typically 1 year after acquisition).

7. Summary

The long-term legacy of COSMOS: COSMOS is the largest contiguous area ever imaged by HST. It is likely to remain for the next decades the largest area imaged in the optical at better than 0.05 arcsec resolution, well through the JWST era. As such, it is destined to represent the reference field for future studies of observational cosmology, attracting massive time investments by every new facility coming on line, e.g., ALMA, Herschel, JWST, etc. While we have expanded on several immediate scientific goals of the project we believe that the long-term legacy of COSMOS will allow scientific applications well beyond those listed in the present paper.

We gratefully acknowledge the contributions of the entire COSMOS collaboration consisting of more than 70 scientists. The HST COSMOS Treasury program was supported through NASA grant HST-GO-09822. The COSMOS Science meeting in May 2005 was supported in part by the NSF through grant OISE-0456439.

Facilities: HST (ACS), HST (NICMOS), HST (WFPC2), Subaru (Scam), NRAO (VLA), XMM, GALEX, Spitzer (IRAC), Spitzer (MIPS), CFHT, UKIRT, CSO, IRAM (30m).

REFERENCES

- Adelberger, K. et al. 1998, ApJ, 505 18
Adelberger, K. et al., ApJ, 619, 697
Aguirre, J. et al. 2006, ApJS, this volume

- Ajiki, M. et al. 2006, ApJS, this volume
- Bahcall, N. et al. 2004, ApJ, 603,1
- Beckwith, S. V. B.. et al. 2006 (in preparation)
- Bell, E., Wolf, C., Meisenheimer, K., Rix, H-W, Borch, A.,Dye, S., Kleinheinrich, M.,
Wisotzki, L. & McIntosh, D. H. 2004, ApJ, 608, 752
- Benson, A. J., Frenk, C. S., Baugh, C. M., Cole, S. & Lacey, C. G. 2001, MNRAS, 327, 1041
- Bertoldi, F. et al. 2006, ApJS, this volume
- Blain, A. W. et al., 2004, ApJ, 611, 725
- Brusa, M. et al. 2006, ApJS, this volume
- Burgasser, A. et al. 2002, ApJ, 564, 421
- Capak, P. et al. 2006, ApJS, this volume
- Capak, P. et al. 2006, ApJS, this volume
- Cappellutti, N. et al. 2006, ApJS, this volume
- Cassata, P. et al. 2006, ApJS, this volume
- Chary, R. & Elbaz, D., ApJ, 556, 562
- Cimatti, A., et al.2004, Nature, 430, 184
- Cristiani, S. et al. 2004, ApJ, 600, 119.
- Conselice, C. et al. 2004, ApJ, 600, L139
- Croom, S.M., Warren, S.J. & Glazebrook, K. 2001, MNRAS, 328, 150
- Daddi, E., et al. 2000, A&A, 361, 535
- Eales, S., Lilly, S., Gear, W., Dunne, L., Bond, J. R., Hammer, F., Le Fvre, O., & Crampton,
D., 1999, ApJ, 515, 518
- Ettori, S., Tozzi, P., Borgani, S. & Rosati, P. 2004, \dot{a} , 417, 13
- Fassnacht, C. et al. 2004, ApJ, 600, L155
- Ferguson, H.C. et al. 2000, ARA&A, 38, 667

- Ferguson, H.C. et al. 2004, ApJ, 600, 107
- Finoguenov, A. et al. 2006, ApJS, this volume
- Frenk, C. et al. 2002, astro-ph/0007362
- Fukugita, Hogan & Peebles, 1998, ApJ, 503, 518
- Giavalisco, M et al. 1998, ApJ, 503, 543
- Giavalisco, M. et al. 2004, ApJ, 600, 99
- Giavalisco, M. et al. 2006, ApJ, this volume
- Gilli, B. et al. 2003, ApJ, 592, 721
- Glazebrook, K. et al. 2004, Nature, 430, 181
- Hasinger, G. et al. 2006, ApJS, this volume
- Hernquist, L. & Springel, V. 2003, MNRAS, 341,1253
- Impey, C. D. et al. 2006, ApJS, this volume
- Kaiser, N. et al. 1995 ApJ, 449, 465
- Labbé, I. et al. 2003, AJ, 125, 1107
- Lilly, S. J.,Le Fevre, O., Hammer, F. & Crampton, D. 2006, ApJ, 460, L1
- Lilly, S. et al. 2006, ApJS, this volume
- Madau, P.,Ferguson, H. C., Dickinson, M. E., Giavalisco, M.,Steidel, C. C. & Fruchter, Andrew MNRAS, 283, 1388
- Massey, R. J. et al. 2006, ApJS, this volume
- Mei, S. et al. 2006, ApJ, 639, 81
- Mellier, Y. 1999, ARA&A, 37, 127
- Mobasher, B. et al. 2006, ApJS, this volume
- Park, Y. et al. 2004, ApJ, 600, 155
- Peebles, J.E., 2002, ASPC, 283, 351

- Refregier, A. 2003, *ARA&A*, 41, 654.
- Renzini, A. 2006, *ARA&A*, 44, in press (astro-ph/0603479)
- Rhodes, J. R. et al. 2006, *ApJS*, this volume
- Rix, H.-W. et al. 2004, *ApJS*, 152, 163.
- Sanders, D. et al. 2007, (in preparation)
- Scarlata, C. et al. 2006, *ApJS*, this volume
- Schinnerer, A. et al. 2006, *ApJS*, this volume
- Schiminovich, D. et al. 2006, *ApJS*, this volume
- Scoville, N. et al. 2006a, *ApJS*, this volume
- Scoville, N. et al. 2006b, *ApJS*, this volume
- Shapley, A. et al. 2001, *ApJ*, 562, 95
- Smail, I. et al. 2002, *MNRAS*, 331, 795
- Smith, G. 2002, *MNRAS*, 330, 1
- Springel, V. et al. 2006, astro-ph-0504097
- Steidel et al. 2004, *ApJ*, 604, 534
- Taniguchi, Y. et al. 2006, *ApJS*, this volume
- Taniguchi, Y. et al. 2006a, *ApJS*, this volume
- Williams, R. E. et al. 1996, *AJ*, 112, 1335.
- Williams, R. E. et al. 2000, *AJ*, 120, 2735.

Table 1. Expected Numbers of Objects in COSMOS $2\pi^\circ$ Field

Class	#	I_{AB} (10σ)	Reference
Galaxies	3.0×10^6	< 27.5	COSMOS-Subaru : Taniguchi et al. (2006)
Galaxies	1.9×10^6	< 27	COSMOS-HST : Scoville et al. (2006a)
Galaxies	300,000	< 25	COSMOS : Scoville et al. (2006a), Taniguchi et al. (2006)
XMM-AGN	~ 2000	5×10^{-16} cgs	XMM-COSMOS: Hasinger et al. (2006); Cappelluti et al. (2006)
XMM-clusters	~ 120	1×10^{-15} cgs	XMM-COSMOS : Finoguenov et al. (2006)
strong lens systems	60–80		Fasnacht et al. (2004)
Galaxies w/ Spectra	$\sim 5 \times 10^4$	$I \leq 25$	z-COSMOS : Lilly et al. (2006); Impey et al. (2006)
QSOs	600(100)	24(21)	Croom et al. (2001)
$z > 4$ QSOs	50	25	Cristiani et al. (2004)
ULIRGs	3,000	26	Smail et al. (2002)
ExtremelyRedObjects	25,000	25	Daddi et al. (2000); Smith (2002)
LymanBreakGalaxies ($z \leq 2$)	65,000	25.5	Steidel et al. (2004)
LymanBreakGalaxies ($z \sim 3$)	10,000	25.5	Shapley et al. (2001)
Red high- z Galaxies ($z > 2$)	10,000	25.5	Labbé et al. (2003)
L,T Dwarfs	300(< 200 pc)	28(4σ)	Burgasser et al. (2002)
KuiperBeltObjects	100-250	27	S-COSMOS Sanders et al.(2007)

Table 2: Infrared Backgrounds and Sensitivities (1600 sec)

Field	$8\mu\text{m}$		$24\mu\text{m}$		$100\mu\text{m}$
	Background MJy/sr	$S_\nu(5\sigma)$ μJy	Background MJy/sr	$S_\nu(5\sigma)$ mJy	Background MJy/sr
COSMOS	6.9	12.7	37	0.080	0.90
Lockman, CDF-S	5.0-5.3	11.0	18.4-19.4	0.061	0.45
SWIRE-XMM	7.1	12.9	31.1	0.078	1.25

Note. — Background estimates obtained using the Spitzer Science Center (SSC) Spot program. Sensitivity estimates for 1600 sec of integration obtained using the SSC Sens-Pet program and interpolating to the specified background level, scaling as the square root of the background.

Table 3. Multi- λ COSMOS Data

Data	Bands / λ / Res.	# Objects	Sensitivity ^a	Investigators	Time
HST-ACS	814I		28.8	Scoville et al.	581 orbits
HST-ACS	475g		28.15	Scoville et al.	9 orbits
HST-NIC3	160W		25.6(6% area)	Scoville et al.	590 orbits
HST-WFPC2	300W		25.4	Scoville et al.	590 orbits
Subaru-SCam	B, V, r', i, z', g'		28 - 26	Taniguchi et al.	10 n
Subaru-SCam	10 IB filters		26	Taniguchi Scoville	11 n
Subaru-SCam	NB816		25	Taniguchi et al.	8 n
CFHT-Megacam	u*		27	Sanders et al.	24 hr
CFHT-Megacam	u,i*		26	LeFevre et al.	12 hr
CFHT-LS	u-z			Deep LS Survey	
NOAO/CTIO	K _s		21	Mobasher et al.	18 n
CFHT/UKIRT	J,H,K		24.5–23.5	Sanders et al.	12 n
UH-88	J		21	Sanders et al.	10 n
GALEX	FUV,NUV		26.1,25.8	Schminovich et al.	200 ks
XMM-EPIC	0.5 – 10 keV		10 ⁻¹⁵ cgs	Hasinger et al.	1.4 Ms
CXO	0.5 – 7 keV			Elvis et al.	future
VLT-VIMOS sp.	R=200	3000	I<23	Kneib et al.	20 hr
VLT-VIMOS sp.	R=600	20000	I<22.5, 0.1 ≤ z ≤ 1.2	Lilly et al.	600 hr
VLT-VIMOS sp.	R=200	10000	B<25, 1.4 ≤ z ≤ 3.0	Lilly et al.	600 hr
Mag.-IMAX sp.	R=3000	2000		Impey, McCarthy, Elvis	12 n
Keck/GEMINI sp.	R=5,000	4000	I<24	Team Members	
Spitzer-MIPS	160,70,24 μ m		17,1,0.15 mJy	Sanders et al.	392 hr
Spitzer-IRAC	8,6,4.5,3 μ m		11,9,3,2 μ Jy	Sanders et al.	220 hr
IRAM-MAMBO	1.2 mm		1 mJy (20 \times 20')	Bertoldi et al.	90 hr
CSO-Bolocam	1.1 mm		3 mJy	Aquirre et al.	40 n
JCMT-Aztec	1.1 mm		0.9 mJy (1 σ)	Sanders et al.	5 n
VLA-A	20cm		7 μ Jy(1 σ)	Schinnerer et al.	60 hr
VLA-A/C	20cm		10 μ Jy(1 σ)	Schinnerer et al.	275 hr
SZA(full field)	9 mm		S-Z to 2 \times 10 ¹⁴ M _⊙	Carlstrom et al.	2 mth

^aSensitivities are AB mag and 5 σ for a point sources unless noted otherwise.

Table 4. COSMOS Data Archives and Websites

Location	Contents	URL
COSMOS website	project & science webpages + links	http://www.astro.caltech.edu/\$\sim\$cosmos/
COSMOS archive (IPAC/IRSA)	Imaging : HST, Subaru, NOAO, CFHT, UH, UKIRT , XMM , VLA , GALEX Spectroscopy : VLT-VIMOS, Mag.-IMAX	http://irsa.ipac.caltech.edu/data/COSMOS/
STScI/MAST	Imaging : HST	http://archive.stsci.edu/
INAF - IASF Milano	Data Tools & Archive	http://cosmosdb.mi.iasf.cnr.it
Obs. Marseille	Spectroscopy Archive	http://cencosw.oamp.fr/EN/index.en.html

a

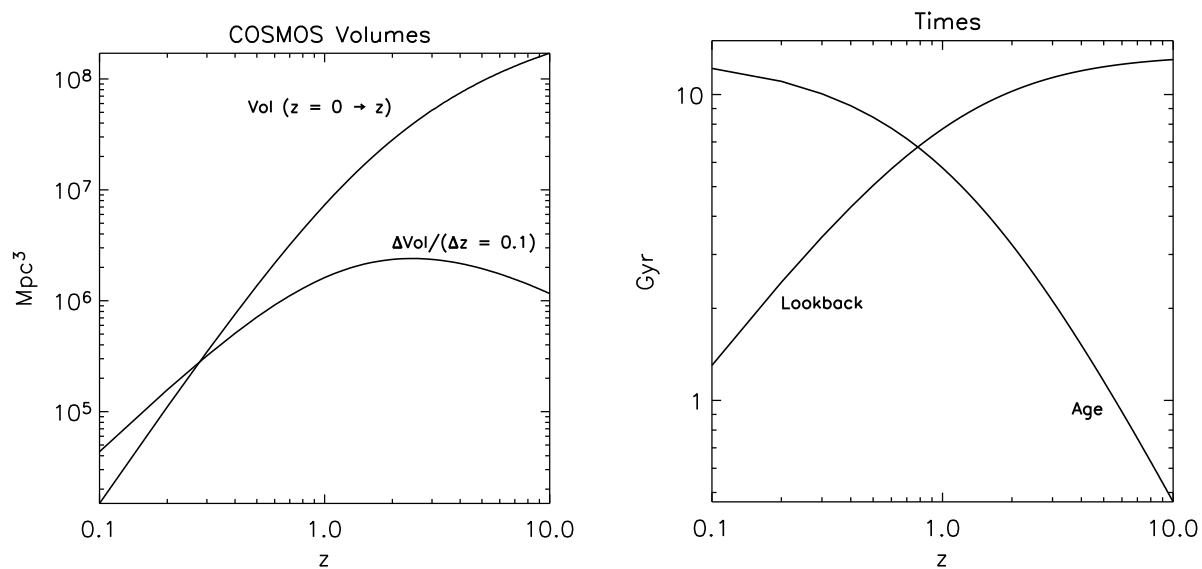


Fig. 1.— **On the left**, the volumes sampled by COSMOS out to redshift z and in a shell of width $\Delta z = 0.1$ for a nominal area of 2 square deg. (The COSMOS ACS imaging covers ~ 1.8 whereas the ground based photometry is complete in most bands over ~ 2.55 square deg.) **On the right**, the cosmic age and lookback times as a function of z for the concordance model ($H_0 = 70 \text{ km s}^{-1} \text{ Mpc}^{-1}$, $\Omega_m = 0.3$ and $\Omega_\Lambda = 0.7$)

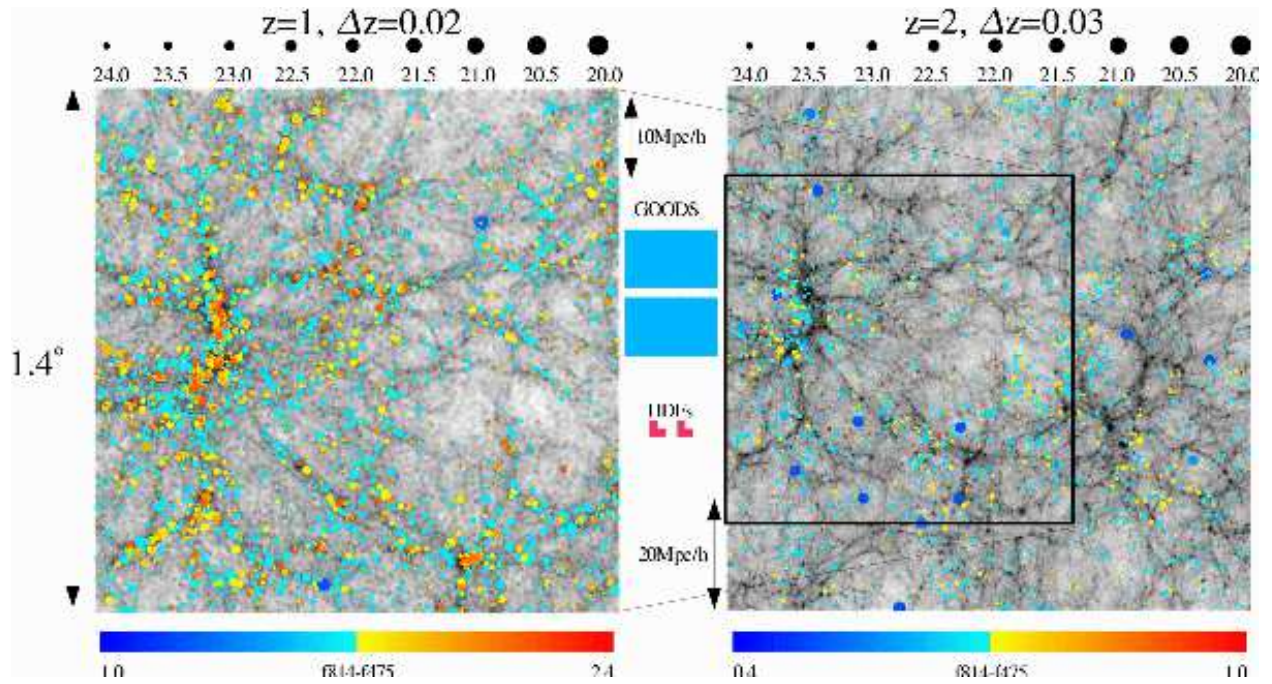


Fig. 2.— Λ -CDM simulation results for 2° at $z = 1$ and 2 , illustrating the scales of voids and wall regions and the ‘expected’ correlation of galaxy evolution with environmental density (Frenk et al.2002). The gray-scale indicates the dark matter distribution and the symbols show magnitudes of galaxies computed for I-band. The depth of the redshift slice is $\Delta z = 0.02$ (50 Mpc at $z = 1$). Also shown are the HDF and GOODS field sizes ; the GEMS field size is $1/4^\circ$.

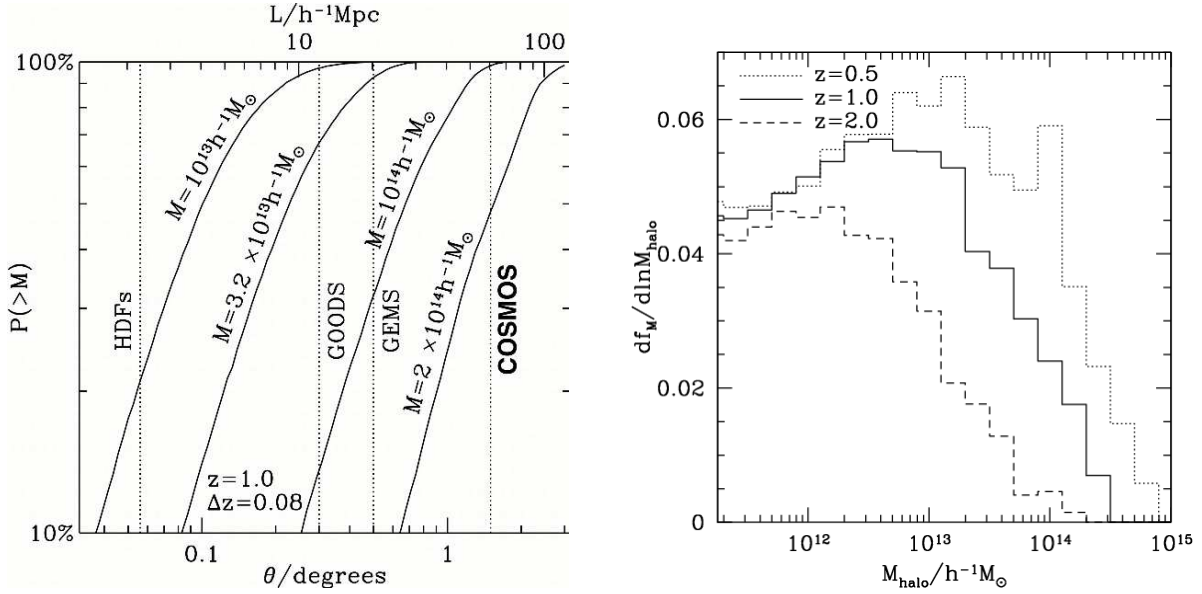


Fig. 3.— **On the left**, the probability of enclosing at least one structure of the specified mass is shown as a function of the field size at $z = 1$ from the Virgo consortium Λ -CDM simulation (Frenk et al.2002). The masses shown correspond approximately to : the Local group, a ‘poor’ cluster, Virgo and about 30% of Coma. **On the right**, the distribution of halo masses is shown for $z = 0.5, 1$ and 2 , illustrating the expected (but not yet verified) evolution in the halo and cluster mass distributions from the Λ -CDM simulation (Frenk et al.2002). $\Delta z \simeq 0.08$ was chosen only to have a significant probability of including a massive structures, but $\Delta z \simeq 0.02$ is required to resolve structures in the line of sight.